J Solid State Electrochem (2007) 11:1183–1190
DOI 10.1007/s10008-006-0258-0

ORIGINAL PAPER

Impedance modelling of two-phase solid-state ionic conductors. Part II—application to high-lithium-content $x\mathrm{Li_2O}$–$\mathrm{B_2O_3}$ fast-ion conducting glasses

E. E. Horopanitis · G. Perentzis · L. Papadimitriou

Received: 27 June 2006 / Revised: 29 November 2006 / Accepted: 8 December 2006 / Published online: 16 January 2007

Abstract The equivalent circuit model of two-phase ionic conductors, introduced in Part I of this work, was applied to a set of $x\mathrm{Li_2O}$–$\mathrm{B_2O_3}$ fast-ion conducting glasses, with x ranging from 3.0 to 4.5. The shape of Arrhenius plots, constructed by equivalent circuit fitting of impedance spectra measured at various temperatures, turned out to be in agreement with the predictions of the model. The analysis procedure, which was developed by mathematical investigation in accordance with the implications of the model, was employed to determine the activation energies of the two present phases and the total DC ionic resistivity of the examined glasses.

Keywords Ionic conductivity · Impedance spectroscopy · Equivalent circuits · Lithium borates · Glasses

Introduction

In the previous first part of this work, an equivalent circuit was introduced as an electrical model to be applied to solid-state ionic conductors, composed of two distinctly separated phases. The configuration of the circuit was decided upon physical arguments, based largely on a corresponding micrometer-scale structure of the two-phase material. One of the constituent phases is considered to be dispersed in the form of suspended islands within the second phase, which forms the background of the material structure.

E. E. Horopanitis · G. Perentzis · L. Papadimitriou (✉)
Section of Solid State Physics, Department of Physics,
Aristotle University of Thessaloniki,
54124 Thessaloniki, Greece
e-mail: pleonida@auth.gr

The electrical properties of ionic conductors are evaluated by employing impedance spectroscopy [1]. The use of equivalent circuits is a necessary means of interpreting impedance spectra and subsequently calculating the conductivity of any ionic conductor. The purpose of developing the model for two-phase materials was to account for the complex dual-slope behavior observed in the Arrhenius plots, resulting from customary interpretation of impedance measurements performed under variable temperature conditions.

In the present second part, the model is applied to a set of heavily lithiated boron oxide samples, and its validity is verified. Lithiated boron oxides $x\mathrm{Li_2O}$–$\mathrm{B_2O_3}$ are a class of vitreous fast-ion conductors, which have been investigated to be utilized as solid electrolytes in a wide variety of applications [2–4]. Boron oxide ($\mathrm{B_2O_3}$) is the glass network former. When doped with lithium oxide ($\mathrm{Li_2O}$), which acts as the network modifier, mobile lithium ions are introduced in the vitreous host material, giving rise to ionic conductivity. If the network modifier and former are mixed during synthesis by a large molar ratio, roughly for $x>2$, then it turns out that crystalline islands are formed against the background of the vitreous network structure [4]. The resulting inhomogeneity in so heavily lithiated boron oxide glasses conforms to the assumptions regarding the structure of the two-phase material, for which the proposed equivalent circuit model is to be applied.

A series of high-lithium-content $x\mathrm{Li_2O}$-$\mathrm{B_2O_3}$ glass samples were prepared, with $x=3.0$ to $x=4.5$, to the purpose of validating the proposed model. Their structure was determined by employing scanning electron microscopy (SEM), and their electrical properties were investigated by impedance spectroscopy. The measured impedance spectra at various temperatures were analyzed, and the resulting Arrhenius plots were evaluated to derive the ionic conduc-

tivity activation energy of the vitreous and crystalline constituent phases, according to the procedure that is implied by the predictions of the model and described in detail in the first part of this work. Finally, the feasibility of extracting quantitative results, regarding the microscopic properties of the individual phases, is briefly discussed.

Materials and methods

The lithiated boron oxide fast-ion conductors of stoichiometry xLi_2O–B_2O_3, with x ranging from 3.0 to 4.5, were prepared by melting appropriate quantities of reagent-grade Li_2CO_3 and B_2O_3 precursor materials and quenching the melt by pressing between steel plates. Carbon is removed from the melt in the form of gaseous CO_2, which is released during the thermal decomposition of Li_2CO_3 to Li_2O. The samples produced by this procedure are shaped in the form of sheets with thickness of the order of 1 mm. Details on the preparation of the samples have been reported elsewhere [4].

The presence of suspended crystalline islands, scattered throughout the glassy background in all the samples, is evident even to the naked eye. Depending on the cooling rate from the molten state, the density of the formed crystallites varies, but in general, an increase in the sample lithium content implies an according increase in the size and density of the dispersed islands of the crystalline phase. Moreover, there is a distinct differentiation between the samples of lower lithium content, x=3, x=3.5, and x=3.75, and those of higher lithium content, x=4 and x=4.5. As far as the lower-lithium-content glasses are concerned, the background vitreous phase is clear and transparent, whereas the individual grains of the crystalline phase are easily distinguishable and can be told apart even without the use of instruments. On the contrary, the higher-lithium-content samples show a very dense dispersion of crystallites, indicated by the milky-white semi-transparent appearance of the background phase [4]. This differentiation with respect to the material lithium content has a direct impact on the shape of the Arrhenius plots obtained from the samples, as will be shown later on.

For impedance measurements to be performed, ohmic contacts were provided on either side of the sample sheets by thermal evaporation of gold. The developed gold electrodes are known to be blocking to lithium ions [2]. Silver paint was used to connect the electrodes to the lead wires of the experimental probe. Impedance spectra were recorded by an Autolab modular electrochemical instrument, equipped with PGSTAT30 potentiostat and galvanostat and FRA2 frequency response analyzer (Eco Chemie, The Netherlands). Data analysis and equivalent circuit fitting were carried out by using the software accompanying the instrument. During the measurements, the samples were kept in a vacuum of the order of 1 Pa and under very stable temperature conditions. The samples were heated in a glass tube that was inserted in a cylindrical furnace, controlled by an analogue temperature controller (Stanton Redcroft, UK).

Results and discussion

The SEM pictures of two samples, x=3.5 and x=4.5, are shown in Fig. 1, where the considered micrometer-scale structure of the two-phase material is confirmed. The crystalline phase is suspended throughout the bulk vitreous phase in the form of isolated grains. The higher density of the scattered crystallites in the higher-lithium-content samples is also demonstrated.

Three typical impedance spectra, obtained from the x=3.75 sample at three different temperatures, are displayed in Nyquist representation in Fig. 2. They consist of two consecutive semicircular arcs, appearing toward each

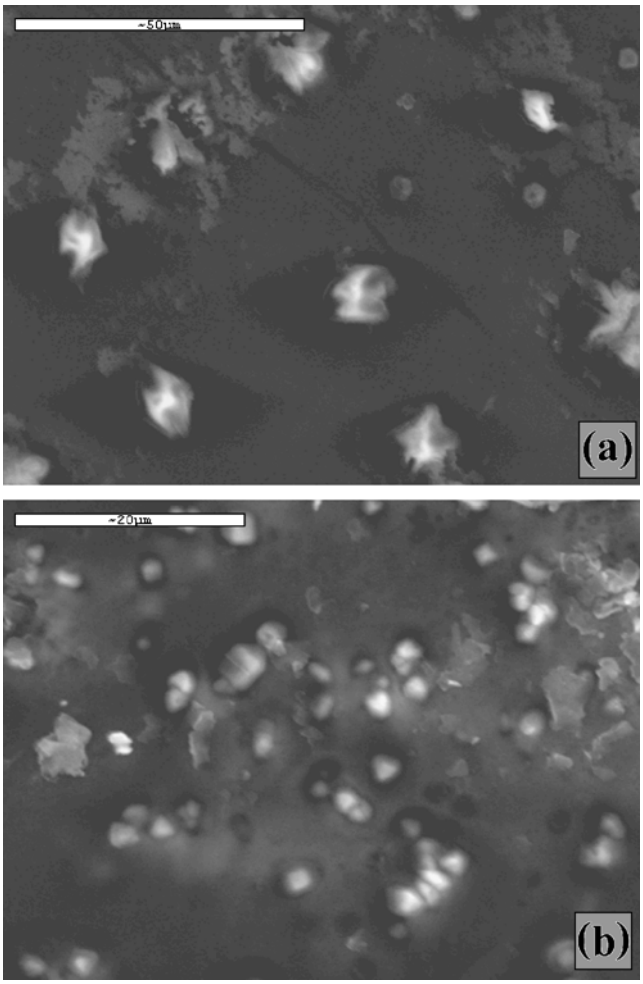

Fig. 1 SEM pictures of the x=3.5 (**a**) and x=4.5 (**b**) samples

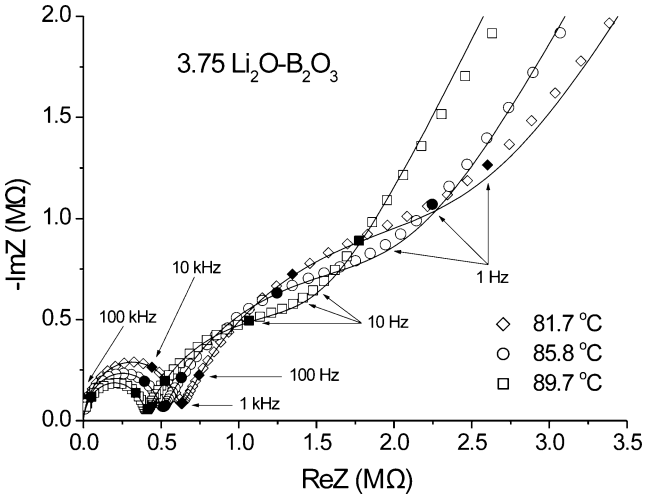

Fig. 2 Impedance spectra obtained from the x=3.75 sample, demonstrating the variation with temperature of the radii of the semicircular arcs in the Nyquist plot

spectrum's high-frequency branch, and a straight line in the low-frequency branch. The straight line is a direct consequence of the polarization of the ion-blocking interfaces between the sample and the electrodes, occurring at low frequencies. The formation of two arcs, at high and intermediate frequencies, is characteristic of two-phase systems. Each arc is attributed to an electrical relaxation process, each of which, in turn, is thought of as being due to each phase present in the system. With increasing temperature, the radius of both arcs decreases, indicating a corresponding decrease in the resistance that the ionic conductor exhibits to the flow of current. Naturally, the ionic resistivity of both the phases is expected to decrease with temperature. Mixed ionic and electronic conductors are also known to yield impedance spectra similar to those of two-phase systems [5, 6], but such is not the case, as lithium borates have long been known to be purely ionic conductors [2, 3].

There is an important experimental restriction that has to be mentioned, concerning the useful temperature range covered in impedance measurements. Most solid-state ionic conductors exhibit very low conductivity at room temperature in comparison to other types of conductors, several orders of magnitude smaller than the conductivity of semiconductors [2]. Fast-ion conductors are an exception to this general statement, and conductivity values as high as the order of 10^{-3} S/cm have been attained at room temperature [2]. Impedance measurements, in effect, are usually carried out at elevated temperatures. The lithiated boron oxide systems with heavy lithium doping that are being investigated exhibit high ionic conductivity, such that the impedance of sample sheets about 1-mm thick is measurable even at room temperature [4]. The complication that arises is that, at low temperatures, the impedance of the experimental cell at low frequencies reaches the limits of the frequency response analyzer accuracy. In consequence, the measured spectra turn out to be very noisy, and, moreover, the equivalent circuit parameters determined by non-linear least squares fitting are accompanied by large uncertainty factors. Of course, the electrical and electrochemical noise may be suppressed by a proper selection of measuring equipment and experimental cells. Due to the above limitation, impedance measurements were not performed at or below room temperature, and the lower temperature limit for each sample was set by the specifications on the range and accuracy of the available instrumentation.

In addition, there is an upper temperature limit, dictated by phenomenology. With increasing temperature, the conductivity of the material system increases, resulting in a corresponding decrease in the size of the semicircular arcs seen in the impedance spectrum Nyquist plot. It turns out that, for a given change in temperature, the percentage of change in the radius of the second arc, observed at lower frequencies, is larger than the respective change in the radius of the first arc, observed at higher frequencies. This relative tendency is shown in Fig. 3, which contains impedance spectra obtained from the x=3.75 sample at various temperatures. The spectra have been normalized to the diameter of the first arc. Normalization was carried out by dividing both the real and imaginary parts of the impedance by the resistance value, as turned out by fitting, that is associated with the high-frequency arc. In this way, the Nyquist plots at different temperatures were scaled down to common axes, thus allowing direct comparison of the relative size of the component arcs with increasing temperature. It can be seen that, as the temperature increases, the size of the second arc in relation to the size

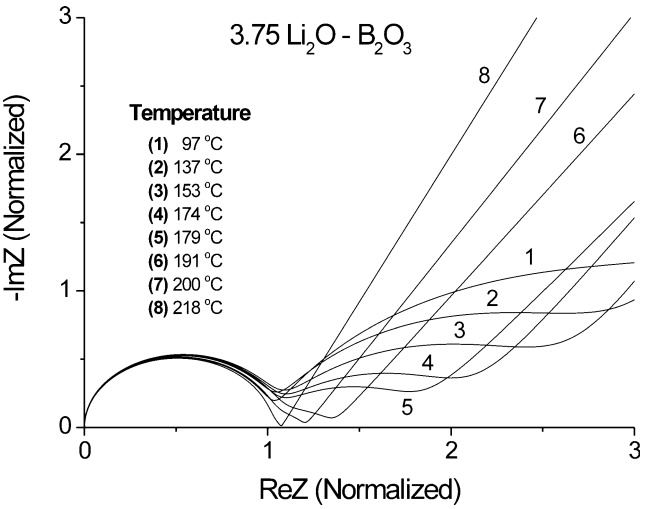

Fig. 3 Impedance spectra in Nyquist representation, obtained from the x=3.75 sample at various temperatures and normalized to the diameter of the high-frequency semicircular arc

of the first arc gradually decreases until, finally, the arc vanishes completely. As the two arcs are attributed to the presence of two phases in the material, it follows from an empirical point of view that, above a certain temperature, the properties of one of the constituent phases are concealed from impedance data.

The useful temperature range, in which quantitative results can be derived out of impedance spectra, was not the same for all the samples. The extreme temperature limits, between which all of our measurements have been carried out, are 37 and 218 °C.

The model introduced in Part I (Fig. 4 of Part I), as well as the two alternative fitting circuits (Fig. 3b and c of Part I), whose impedance frequency response is identical to that of the model circuit, are shown in Fig. 4, which has been reproduced in the present Part II for the sake of completeness. Resistors R_V and R_C stand for the total DC resistance that the vitreous and crystalline phases, respectively, exhibit to ionic current flow. The circuit contains two parallel branches that include ohmic elements, corresponding to the two distinct ionic conduction possibilities, taking place simultaneously. The ionic charge carriers may migrate through the sample volume either by crossing parts of both the vitreous and crystalline phases or by passing through the vitreous phase alone. Parameter p, dependent on geometrical features of the two-phase system microstructure, is introduced as a means of relating the total DC resistance, R_V and pR_V, respectively, which is exhibited by the parts of the vitreous phase included in the above two alternative parallel conduction paths. In the samples of higher lithium content, the crystalline islands are extremely densely distributed in the vitreous phase, and consequently, the only possible conduction path is through both the phases.

It must be stressed that both the model and its equivalent fitting circuits refer to the properties of the bulk two-phase material alone and not the interfaces between the material and the current-collecting electrodes, which constitute an integral part of the measuring cell. An additional constant phase element (CPE) has to be connected in series to the above circuits for complete fitting of experimental impedance spectra to be accomplished, as is explained in Part I. All analyses in the present Part II were inevitably carried out by taking into account the low-frequency electrode polarization branch of impedance spectra. However, electrode polarization effects are not explicitly discussed because the scope of this work is to concentrate on impedance properties of two-phase materials.

The measured impedance spectra are to be fitted to either the first or the second1 fitting circuit of Fig. 4b and c, including, of course, an appropriate electrode polarization CPE. The solid lines in Fig. 2 represent the fitted responses of these circuits to the measured impedance spectra. The as

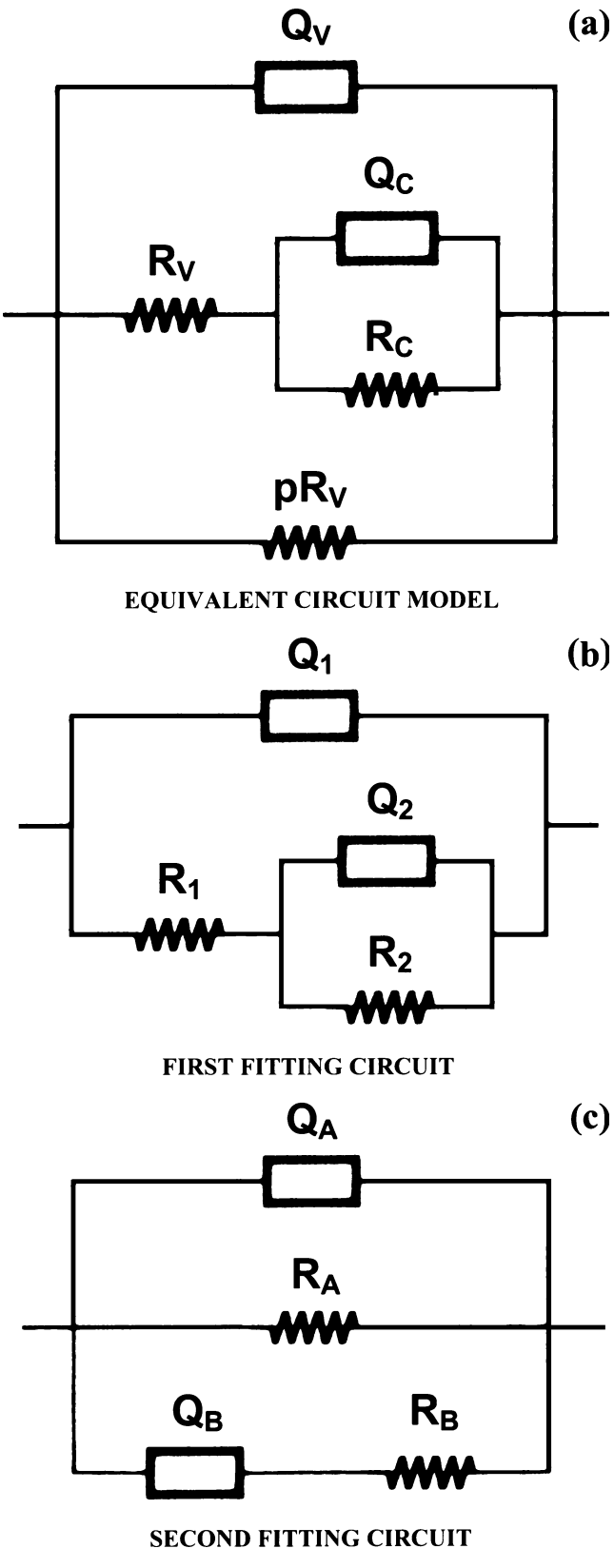

Fig. 4 The equivalent circuit model of two-phase ionic conductors (**a**) and the two alternative fitting circuits (**b**) and (**c**); (Figs. 4, 3b and c, respectively, of Part I of this work)

so determined resistance values R_1, R_2 or R_A, R_B are subsequently converted to the respective conductance values G_1, G_2 or G_A, G_B and plotted in Arrhenius plots. The information regarding the two phases present in the samples is decoupled from the Arrhenius plots by the procedure developed in Part I. Although in theory either one of the fitting circuits would be adequate to analyze experimental impedance data, the use of the first one is advantageous due to the fact that its topology coincides with the model circuit in the extreme limiting case of ionic conduction through both the phases.

The Arrhenius plots of conductances G_1 and G_2, corresponding to resistors R_1 and R_2, respectively, which were calculated by fitting the circuit of Fig. 4b to a series of impedance spectra recorded at various temperatures, are shown in Figs. 5 and 6. The former contains results obtained from the samples of lower lithium content, x=3, x=3.5, and x=3.75, and the latter results from the samples of higher lithium content, x=4 and x=4.5. The values of both R_1 and R_2, returned by the fitting procedure, are fairly accurate. At lower temperatures, the relative error is smaller than 1%. At medium and higher temperatures, the relative error of R_2 increases slightly, apparently due to the gradual decrease in R_2 in relation to R_1, as shown in Fig. 3. Data points of even higher temperature, accompanied by unacceptable error magnitudes, were rejected. It turns out that conductance G_1 always follows an Arrhenius-type dependence on temperature. On the contrary, conductance G_2 does not seem to consistently obey the Arrhenius law, as the samples of lower lithium content, in contrast to those of higher lithium content, do not exhibit a regular change in conductance with changing temperature. The data points of conductance G_2 are lined up in the Arrhenius plot along a curve, which asymptotically tends to two straight lines. The asymptote in the low-temperature limit is characterized by a slope roughly equal to the slope of the straight line, along which the data points of conductance G_1 are aligned. The second asymptote, in the high-temperature limit, is of steeper slope in comparison to the slope of the line in the low-temperature limit. Had the resistors R_1 and R_2 been attributed to the ionic conduction properties of the constituent material phases by one-to-one correspondence, this as so interpreted irregularity in the temperature dependence of the second phase would have been inexplicable.

Let us now briefly summarize the predictions of the proposed model, as far as the first alternative fitting circuit is concerned. Details are given in Part I. When drawn in Arrhenius plots, conductance G_1 data points should always be lined up along a straight line, whereas conductance G_2 data points should be lined up along a curve, which asymptotically tends to two straight lines in the low-temperature and the high-temperature limits. The slope of the low-temperature asymptote should be equal to the slope of conductance G_1 data points' straight line. The ionic conduction activation energy in the vitreous and the

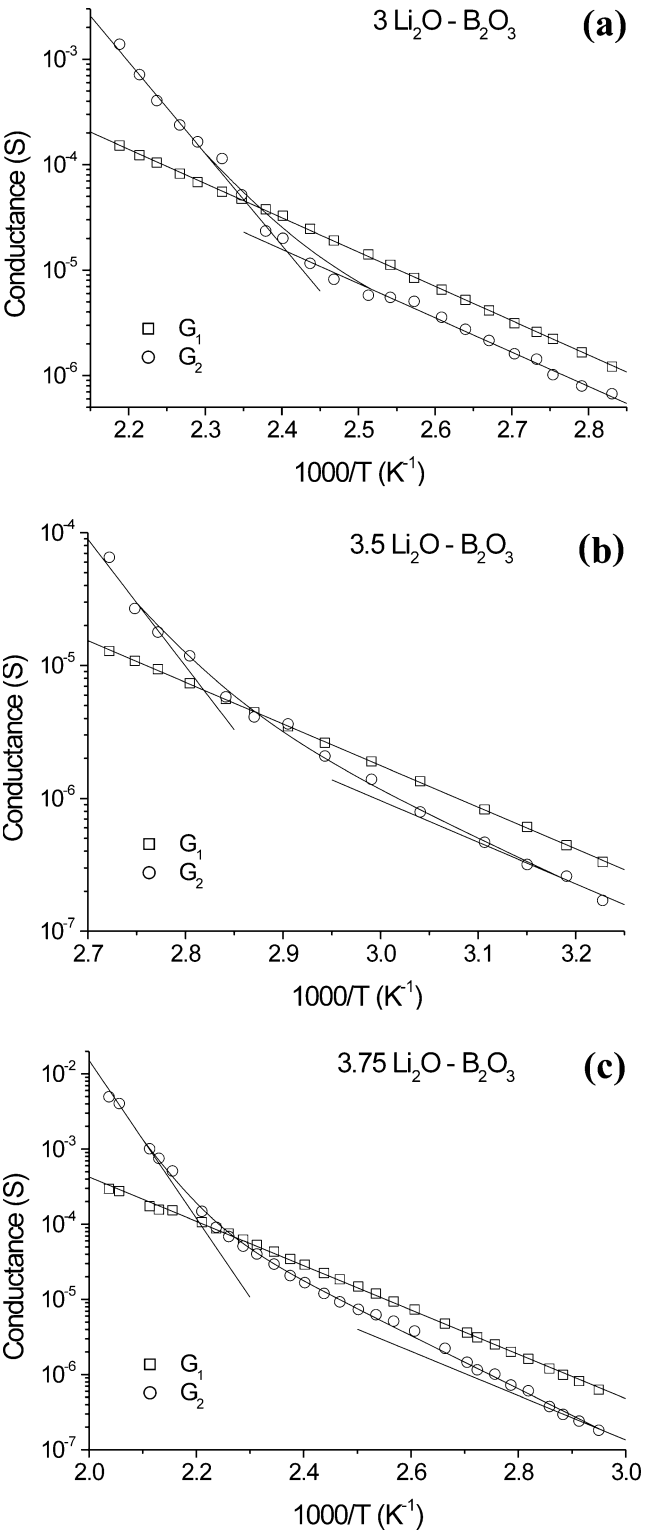

Fig. 5 Arrhenius plots of the lower-lithium-content samples, x=3 (**a**), x=3.5 (**b**), and x=3.75 (**c**), constructed by fitting the circuit of Fig. 4b to the measured impedance spectra

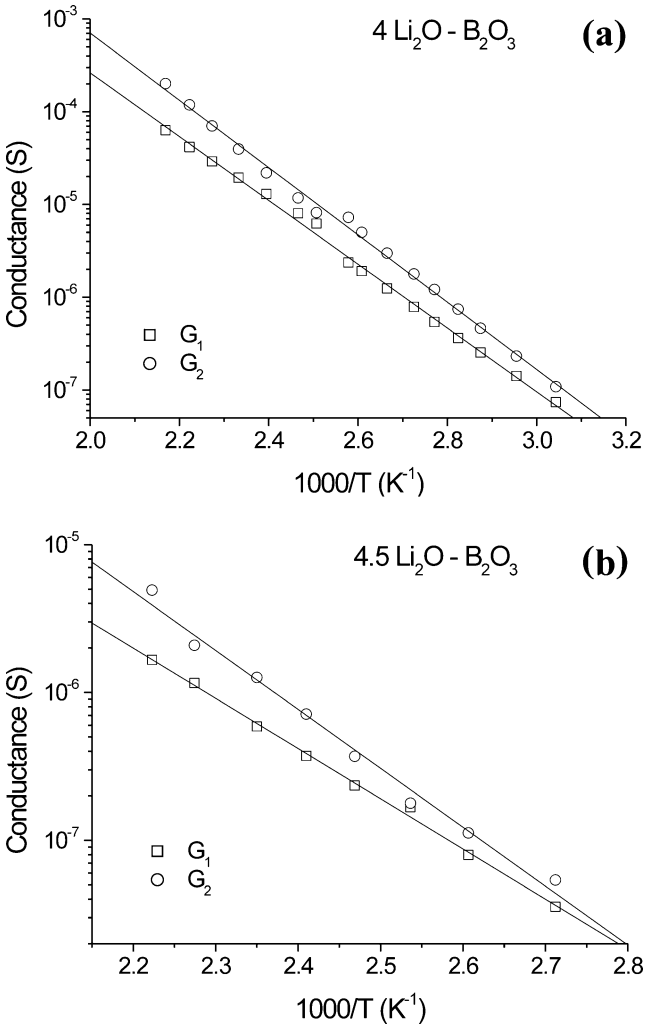

Fig. 6 Arrhenius plots of the higher-lithium-content samples, x=4 (**a**) and x=4.5 (**b**), constructed by fitting the circuit of Fig. 4b to the measured impedance spectra

crystalline phase, E_V and E_C, respectively, may be calculated from the slope of conductance G_1 straight line and conductance G_2 high-temperature asymptote, respectively. In the special case of a material system containing very densely scattered crystalline grains, both conductance G_1 and G_2 data points should be aligned along straight lines, the slopes of which determine the ionic conduction activation energy in the vitreous and crystalline phase, E_V and E_C, respectively. As can be seen in Figs. 5 and 6, the above conclusions are in excellent agreement with the measurements. The solid lines in the figures are simulations of the Arrhenius plots according to the equations derived in Part I, and the calculated activation energies are listed in Table 1. The absolute errors of the listed activation energy values are also contained in Table 1. Only in connection with the lower-lithium-content samples, the crystalline phase activation energy E_C is determined with a comparatively large error, mainly due to the corresponding errors

Table 1 Calculated activation energies and DC ionic resistivities at 25 °C of the lithiated boron oxide samples

x	E_V (eV)	E_V error (eV)	E_C (eV)	E_C error (eV)	ρ_{DC} at 25 °C (Ω·cm)
3	0.642	0.003	1.793	0.133	$2.00 \cdot 10^8$
3.5	0.619	0.002	1.831	0.169	$3.96 \cdot 10^7$
3.75	0.582	0.003	1.925	0.158	$2.31 \cdot 10^8$
4	0.679	0.010	0.716	0.012	$3.93 \cdot 10^8$
4.5	0.671	0.014	0.787	0.033	$1.00 \cdot 10^{10}$

accompanying the high-temperature data points, as has been discussed earlier in this section, as well as the actual curvature of conductance G_2 Arrhenius plots.

Likewise, the predictions of the model regarding the second alternative fitting circuit are as follows. The data points of the sum of conductances $G_A + G_B$ should be lined up along a straight line, the slope of which allows calculation of the vitreous phase activation energy E_V. Conductance G_B data points should be lined up along a curve, which again tends asymptotically to two straight lines in the low-temperature and the high-temperature limits. The slope of the low-temperature asymptote should be equal to the slope of the straight line, along which data points of the sum $G_A + G_B$ are aligned. The differentiation in analysis results, in comparison to the previous case of data returned by the first fitting circuit, is that the slope of the high-temperature asymptote is determined not by the crystalline phase activation energy E_C alone, but by the factor $2E_V$-E_C. If $E_C > 2E_V$, the slope of the high-temperature asymptote is found to be positive, that is, conductance G_B decreases with increasing temperature.

Such is the case in Fig. 7, which contains the Arrhenius plots of conductances $G_A + G_B$ and G_B, calculated by fitting the circuit of Fig. 4c to a series of impedance spectra obtained at various temperatures from the x=3.75 sample. The solid lines in the figure are again simulations of the Arrhenius plots according to the corresponding equations derived in Part I. The calculated activation energies of the material phases are in absolute agreement with those contained in Table 1. It is clear that the proposed equivalent circuit model offers a convenient explanation of the positive slope observed in the successive high-temperature data points of Fig. 7. If, as is customary, conductance G_B had been attributed to the contribution of only the crystalline phase to the total two-phase material impedance response, the positive slope of the Arrhenius plot at high temperatures would have been unacceptable, because, as so interpreted, it dictates that the crystalline phase conductivity decreases as the temperature increases. Therefore, no physical meaning that is directly linked to single phase properties can be attached to conductance G_B. The decrease in G_B with increasing temperature in the high-temperature limit is

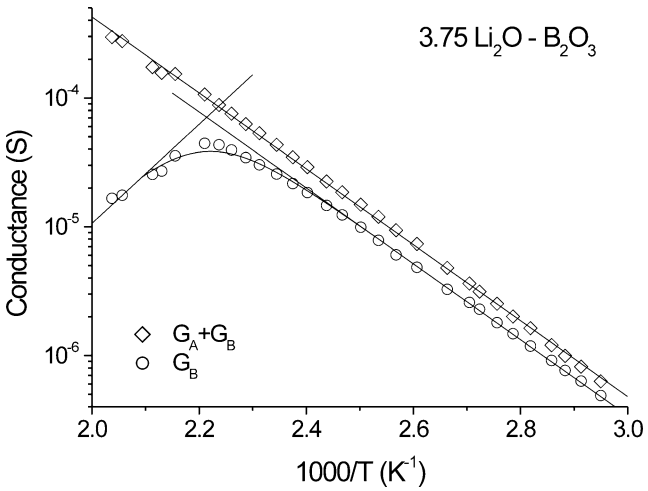

Fig. 7 Arrhenius plots of the x=3.75 sample, constructed by fitting the circuit of Fig. 4c to the measured impedance spectra

clearly a consequence of the transformation laws between alternative equivalent circuits. Instead, the positive slope observed in segments of the Arrhenius plot of G_B is an indication that the second fitting circuit is not by itself a complete model for the two-phase material, but rather a degenerate equivalent circuit derived from an underlying more complex model that represents the true material microstructure in a more realistic way.

In principle, depending on the choice of the first or second fitting circuit, the equations describing the corresponding Arrhenius plots may be simultaneously fitted to the respective sets of data to yield not just the activation energies E_V and E_C, but the pre-exponential factors F_V and F_C and geometrical parameter p as well. In our opinion, determining the values of F_V, F_C, and p for each sample is a matter of no particular significance for the following reasons. Being a mere technical means of crudely relating the microscopic details of the material structure to the macroscopically measurable ionic conductance, the exact values of F_V, F_C, and p contribute very little to a detailed understanding of the nature of the individual constituent phases. Had the micrometer-scale structure of the two-phase system been simple, then calculation of F_V and F_C would have been of some interest because the geometry of the structure would have permitted confident reduction of the ionic conductance pre-exponential factors F_V and F_C to the corresponding ionic conductivity pre-exponential factors. In such an idealized situation, estimation of the ionic conductivity of each phase at any temperature would have been possible according to the Arrhenius equation. In reality, though, the extreme complexity of the actual two-phase material structure, along with the observed large-scale inhomogeneity of the sample sheets, renders any attempt to derive credible values of the ionic conductivity of each single phase a matter of sheer speculation.

What is of practical importance, however, is the total macroscopic DC resistivity of the samples, which can be calculated from the corresponding total DC resistance by taking the sample thickness and the macroscopic surface area of the current-collecting electrodes into account. As can be seen from the topology of the fitting circuits in Fig. 4b and c, the total DC resistance is given by

$$R_{DC} = R_1 + R_2 = \frac{R_A R_B}{R_A + R_B} \quad (1)$$

Because each one of the fitting circuits' resistances participating in the above relation can be evaluated at any temperature with the aid of fitting results, it follows that the total DC ionic resistivity of the samples at room temperature may be calculated. The results are contained in Table 1. The minimum in resistivity is attained for lithium content molar ratio x=3.5, in accordance with previous findings [4].

A few remarks regarding the calculated values of Table 1 are worth pointing out. The classification of the samples into two categories, of lower and higher lithium content, is also revealed in the values of activation energy. Within each category, with increasing lithium content, the vitreous phase activation energy E_V decreases and the crystalline phase activation energy E_C increases, but there is a marked differentiation of the respective values between the two categories. The vitreous phase activation energy is collectively smaller and the crystalline phase activation energy larger in the samples of lower lithium content, in comparison to the samples of higher lithium content. This behavior has to be traced to the composition of each phase. Despite the fact that the two phases are definitely identified in the micrometer scale and give rise to equal in number electrical relaxation time constants resolved by impedance spectroscopy, the presence of local, smaller-scale inhomogeneities is highly likely. Depending on the molar ratio of precursor reagents and preparation conditions, the binary material system Li_2O–B_2O_3 forms vitreous solid solutions in a wide range of compositions [2, 3], as well as nine crystalline single phases [7, 8]. It is possible that several different crystalline phases are simultaneously present in the crystallite grains of the examined samples. Local variations in stoichiometric composition of the vitreous background phase are also possible. In effect, the values of activation energy listed in Table 1 have to be more appropriately treated as average collective values of two phases differentiated in the micrometer scale, rather than true values of strictly defined single phases. It would be ideal, had it been possible to prepare pure phase components, in order to compare fitting results with experimental conductivity and activation energy values directly obtained from independently synthesized single phases. Unfortunately, the molar mixing ratio x of the precursor materials during preparation is beyond the glass-forming region of

the Li_2O–B_2O_3 binary system, attained by the melt-quenching technique [3]. Very recently, the glass-forming region has been extended up to x=5.0, only by employing a special solution method [9] though. On the other hand, it is possible to obtain pure single phases of the various crystalline compounds formed by this particular material system [7]. However, the large number of crystalline phases that are possibly simultaneously present, as well as the evident inhomogeneity of the samples, in density and probably in composition, would make an attempted comparison of phase properties the subject of a separate study. Moreover, it would be very difficult to compare the electrical parameters of samples having the same composition, but different microstructure, because the formation of the crystalline phase is spontaneous during quenching of the melt, and consequently, the volume fraction and grain size of the dispersed crystalline phase cannot be controlled, at least by the implemented quenching technique. But a detailed investigation of the structure and composition of this particular two-phase system is the subject of another work.

Conclusions

A set of high-lithium-content xLi_2O–B_2O_3 ionic conductors were electrically characterized at various temperatures by impedance spectroscopy. The measured spectra were fitted to two alternative equivalent circuits, and the returned values of the circuits' ohmic elements were plotted in Arrhenius plots. The shape of the plots was found to be in excellent agreement with the predictions of the equivalent circuit model introduced in Part I of this work to account for the impedance properties of two-phase materials. The evaluation procedure of Arrhenius plots, dictated by the implications of the model, was applied to yield the activation energies of the constituent phases as well as the total DC resistivity at room temperature of the investigated ionic conductors. All experimental results turned out to support the validity of the proposed two-phase system model.

Acknowledgment This work has been supported by the Greek Ministry of Education through the Pythagoras II research program. Also, the contribution of Lecturer E. Pavlidou for supplying the SEM pictures of Fig. 1 is gratefully acknowledged.

References

1. Macdonald JR (ed) (1987) Impedance spectroscopy emphasizing solid materials and systems. Wiley, New York
2. Julien C, Nazri GA (1994) Solid state batteries: materials design and optimization. Kluwer, Boston
3. Balkanski M (ed) (1991) Microionics: solid state integrable microbatteries. North-Holland, Amsterdam
4. Horopanitis EE, Perentzis G, Pavlidou E, Papadimitriou L (2003) Ionics 9:88
5. Jamnik J, Maier J (1999) J Electrochem Soc 146:4183
6. Jamnik J (2003) Solid State Ionics 157:19
7. Mathews MD, Tyagi AK, Moorthy PN (1998) Thermochim Acta 320:89
8. Meshalkin AB, Kaplun AB (2005) J Crystal Growth 275:e115
9. Banerjee J, Ongie G, Harder J, Edwards T, Larson CR, Sutton S, Moeller A, Basu A, Affatigato M, Feller S, Kodama M, Aguiar PM, Kroeker S (2006) J Non-Cryst Solids 352:674